Subignition Control in the FFHR Helical Reactor

US-Japan Workshop on the Fusion Power Reactor
April 6-7, 2002
at Hyatt Islandia (San Diego, USA)

O.Mitarai (Kyushu Tokai University),
A.Oda (Yatsushiro National College of Technology),
A.Sagara, K.Yamazaki, and O.Motojima (NIFS)

Contents:

1. Ignition control algorithm in FFHR

1.1. 0-dimensional particle and power balance equations

$$\frac{dn_e(0)}{dt} = \frac{1}{(1 - 8 f_O)}\left[(1 + \alpha_n) S_{DT} - \left\{\frac{f_D + f_T}{\tau_p} + \frac{2 f_\alpha}{\tau_\alpha^*}\right\} n_e(0)\right]$$

$$\frac{dn_\alpha(0)}{dt} = (1 + \alpha_n)\; n_D(0)\, n_T(0)\, \eta_\alpha \overline{<\sigma v>_{DT}(x)} - \frac{n_\alpha(0)}{\tau_\alpha^*}$$

$$\frac{dT_i(0)}{dt} = \frac{1 + \alpha_n + \alpha_T}{1.5\, e\, (f_D + f_T + 1/\gamma_i + f_\alpha)\, n_e(0)}\left[P_{EXT}/V_o + \overline{P}_\alpha - (\overline{P}_L + \overline{P}_b + \overline{P}_S)\right]$$

$$- \frac{T_i(0)}{(f_D + f_T + 1/\gamma_i + f_\alpha)}\left[\left(1 - 8 f_O + \frac{1}{\gamma_i} - f_\alpha\right)\frac{1}{n_e(0)}\frac{dn_e(0)}{dt} - \frac{df_\alpha}{dt}\right]$$

where γ_i **= $T_i(0)/T_e(0)$, e = 1.6×10^{-19}**
$\gamma_{DT} = n_D(0)/n_T(0)$,
$f_D = (1-2f_\alpha-8f_O-Zf_{imp})/(1+\gamma_{DT})$
$f_T = \gamma_{DT} f_D$,
$Z_{eff} = (1+\gamma_{DT})\, f_D + 4\, f_\alpha + 64\, f_O + Z^2 f_{imp}$,
$T_i(x)/T_i(0) = T_e(x)/T_e(0) = (1-x^2)^{\alpha_T}$
$n(x)/n(0) = n_\alpha(x)/n_\alpha(0) = (1-x^2)^{\alpha_n}$

ISS95 confinement law: γ_H~1.5 to 1.7 in LHD

$$\tau_{E,ISS95}\ [s] = \gamma_H\, 0.079\; \iota_{2/3}^{0.4}\; \overline{n}_{20}^{\;0.51} \left[\times 10^{19}\ m^{-3}\right] B_o^{0.83}\ [T]$$

$$\overline{a}^{2.21}\,[m]\; R^{0.65}\,[m] \,/\, P_H^{0.59}\ [MW]$$

1.2. External heating power:

This calculation is based on the following experimental facts observed in LHD.

@ No clear transition from L to H mode in LHD.

@ Pellets should be injected to obtain the higher density.

The external heating power is applied to expand the density limit, not to maintain the H-mode regime.

Density limit:

$$\gamma_{DL0}\, n(0) \le n(0)_{lim}\ [m^{-3}] = \frac{0.25\times 10^{20}}{\gamma_{pr}} \sqrt{\frac{\left(\bar{P}_{h,net}\ V_o[MW] x10^{6}\right) B_o[T]}{\bar{a}^2\ R\ [m]}}$$

where

Density limit set value: g_{DL0} **= n(0)$_{lim}$/n(0)= 1.1 > 1.0**

Density limit is slightly higher than the operation density.

Profile factor (g_{pr}**=**$\bar{n}$ **/n(0) = 2/3 parabolic profile),**

External heating power:

$$P_{EXT}(DL)\ [W] = \left(\frac{\gamma_{DL0}\gamma_{pr} n(0)\ [m^{-3}]}{0.25x10^{20}}\right)^2 \frac{R\ \bar{a}^2}{B_o[T]}\, x10^6 - (P_\alpha - P_B - P_S)$$

1.3. Fueling

DT fueling is controlled by the fusion power signal P_f.

Proportional control for pellet injection

$$S_{DT}(t) = S_{DT0} \qquad (\text{ If } e_{DT}(P_f) > 0)$$

$$S_{DT}(t) = 0 \qquad (\text{ If } e_{DT}(P_f) < 0)$$

where

$$e_{DT}(P_f) = \left(1 - \frac{P_f(t)}{P_{fo}(t)}\right)$$

Gain: $G_{f0}(t)$, $S_{DT0} = 1 \times 10^{19}\ m^{-3}/s$
Set value: $P_{fo}(t)$

PID control for continuous gas puffing

$$S_{DT}(t) = S_{DT0}\left\{ e_{DT}(P_f) + \frac{1}{T_{int}}\int_0^t e_{DT}(P_f)dt + T_d\frac{de_{DT}(P_f)}{dt}\right\} G_{fo}(t)$$

Here, PI control was employed.
Integration time: $T_{int} > 20$ sec
Derivative time: $T_d = 0$

1.4. Ignition control diagram

Global ignition control for a helical reactor including the diagnostic and feedback control systems is proposed here.

This diagram is modified from the ITER burn control diagram. (O.Mitarai and K.Muraoka, Fusion Technology, 36 (1999) 194, and Nucl. Fusion, Vol. 39, (1999) 725)

In general, the ignition burn control in a helical system may be easier than a tokamak because the plasma current profile control may not be necessary.

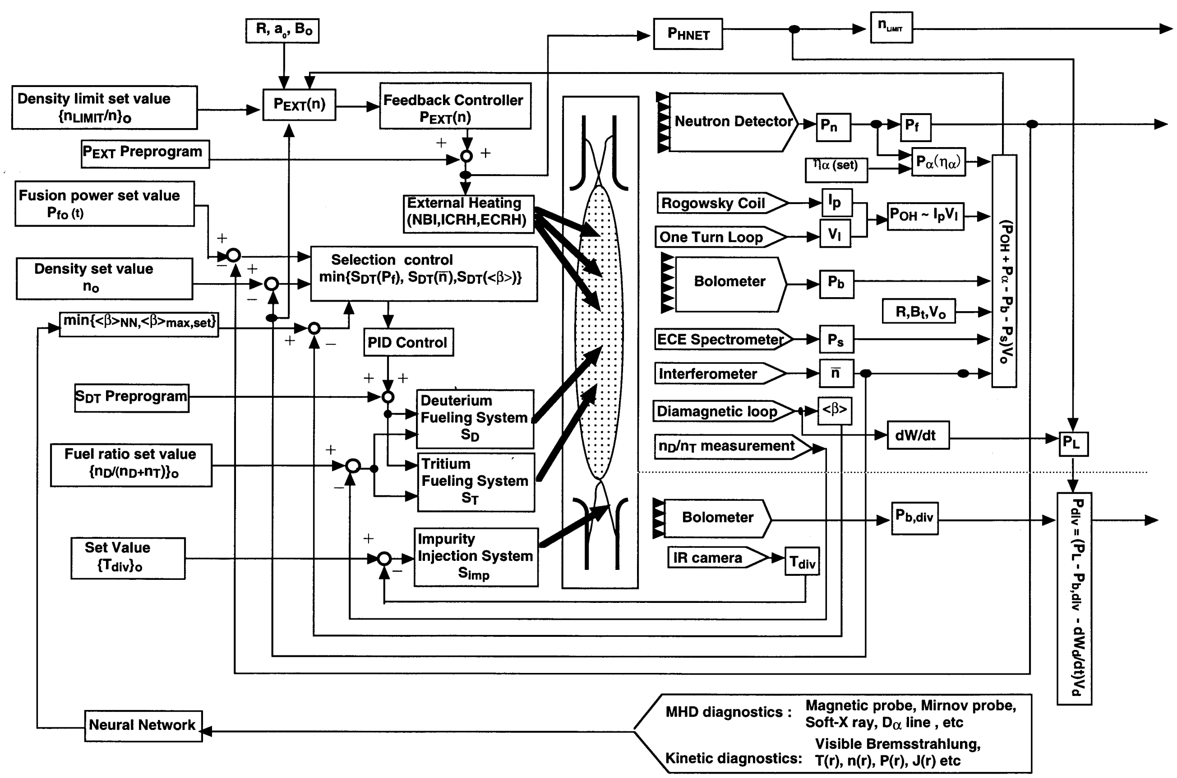

1.5. Parameters

Major radius:	$R = 10$ m
Minor radius:	$a = 1$ m
Magnetic field:	$B_o = 10$ T
Maximum external heating power:	$P_{EXT} = 100$ MW
Enhancement factor over ISS95 scaling :	$\gamma_H = 1.6$
Alpha ash density fraction:	$f_\alpha = 2.1$ %
Oxygen impurity fraction:	$f_O = 0.5$ %
Effective charge:	$Z_{eff} = 1.32$
Alpha confinement time ratio:	$\tau_\alpha^*/\tau_E = 3$
Alpha particle heating efficiency:	$\eta_\alpha = 0.7$
Wall reflectivity and Hole fraction:	$R_{eff} = 0.9$, $f_H = 0.1$
Density and Temperature profile:	$\alpha_n = 1.0$, $\alpha_T = 1.0$

Fusion power	$P_f \sim 1$ GW
Neutron power	$P_n \sim 800$ MW
Alpha loss to the first wall	$P_{\alpha w} \sim 60$ MW
Alpha heating to plasma	$P_{\alpha p} \sim 140$ MW $\}$ $P_\alpha \sim 200$ MW
Bremsstrahlung loss	$P_b \sim 21$ MW
Synchrotron radiation loss	$P_s \sim 9$ MW
Plasma conduction loss	$P_L \sim 110$ MW
Electron density	$n(0) \sim 4.8\text{x}10^{20}$ m^{-3}
Temperature	$T(0) \sim 13$ keV
Beta value	$\langle\beta\rangle \sim 1.6$ %
Average neutron wall loading	$\Gamma_n \sim$ 800MW/434 ~1.84 MW/m^2
Outboard neutron wall loading	$\Gamma_n \sim$ 1.84x1.1~2.0 MW/m^2
Maximum average radiation wall loading	$\Gamma_r \sim$(200+100) MW/434 ~ 0.70 MW/m^2
Maximum outboard radiation wall loading	$\Gamma_r \sim$ 0.70x1.1 ~0.76 MW/m^2
Average radiation wall loading	$\Gamma_r \sim$30 MW/434 ~ 0.07 MW/m^2
Outboard radiation wall loading	$\Gamma_r \sim$0.07x1.1~ 0.08 MW/m^2
Divertor heat load	$\Gamma_r \sim$ 110 MW/($2\pi R$x0.1 m x 4 legs)~4.4 MW/m^2

1.6. Temporal evolution

Subignition access by continuous gas puffing.

control by Density limit , R/a=10/1, B_O = 10 T, γ_H =1.6, S_{DT}(PI)

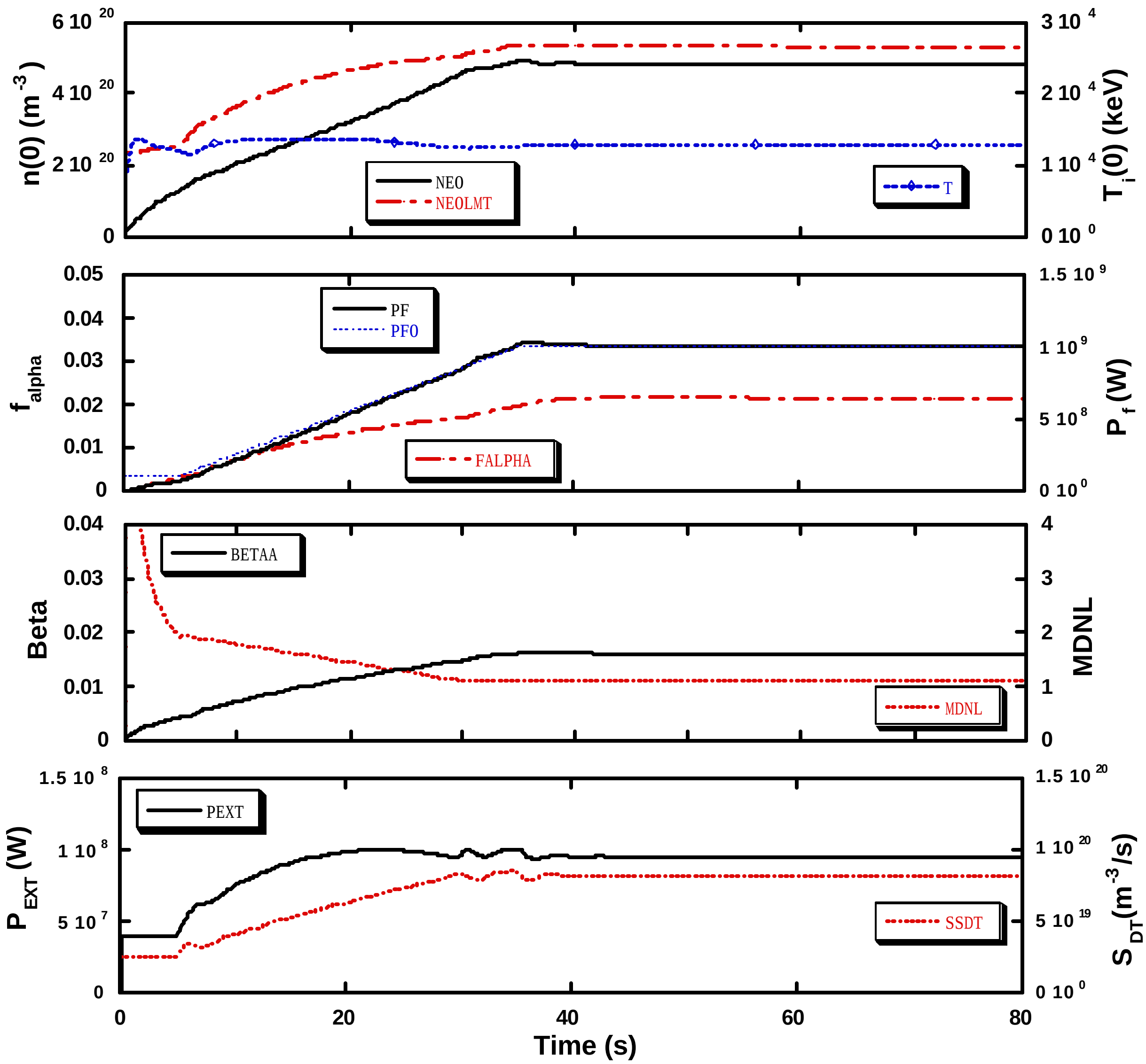

Fig. 1

1.7. Pellet injection algorithm

1.7.1. Pellet pulse generation for simulation

Pellet repetition time: t

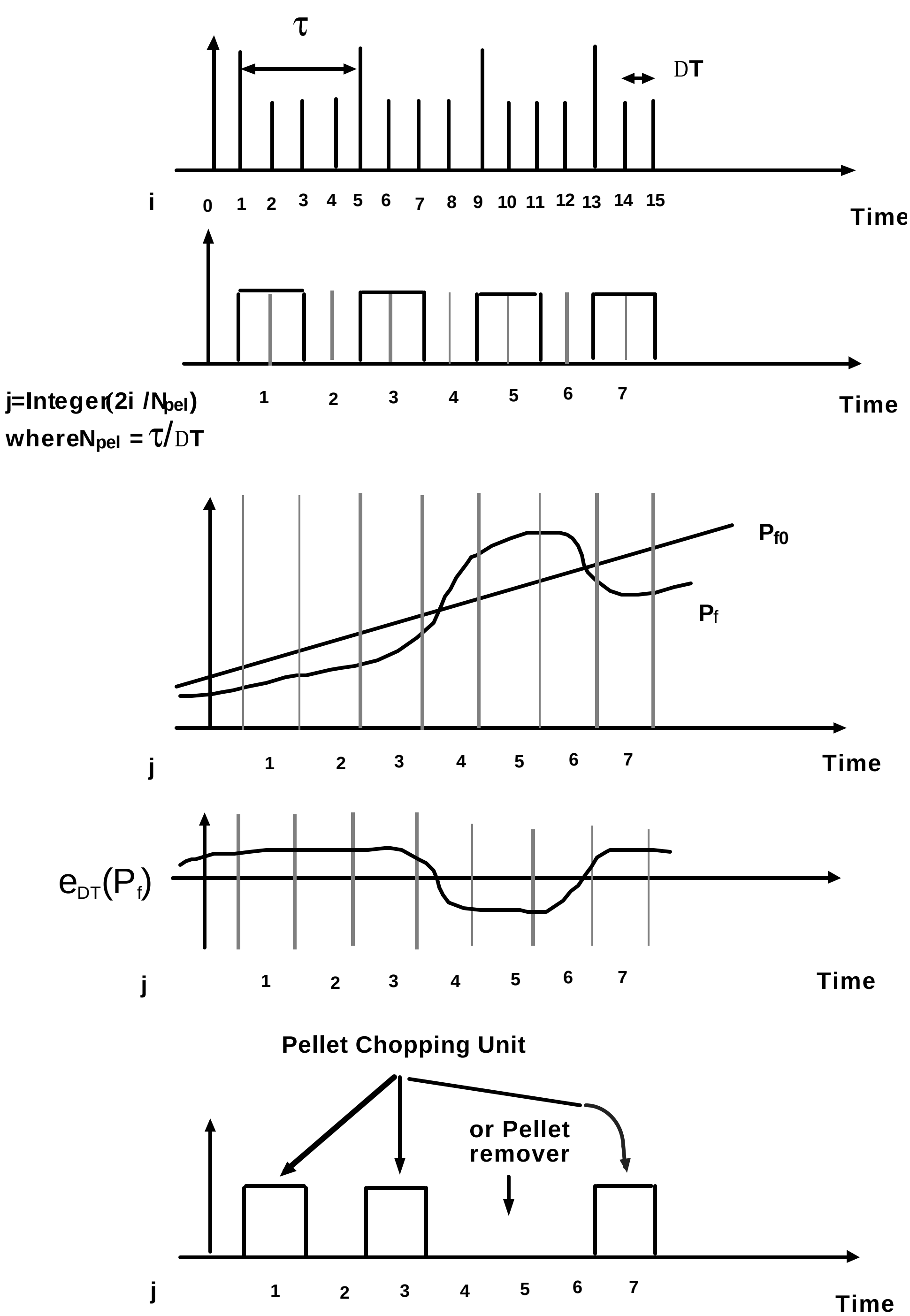

Fig. 2

1.7. 2. Control diagram of pellet injector

@ **Pellet injection algorithm is added to DT gas puffing algorithm.**

@ **DT pellet chopping unit may be controlled by the electric signal, which is generated by the fusion power error signal $e_{DT}(P_f)$.**

@ **If this does not work, the pellet remover should be installed.**

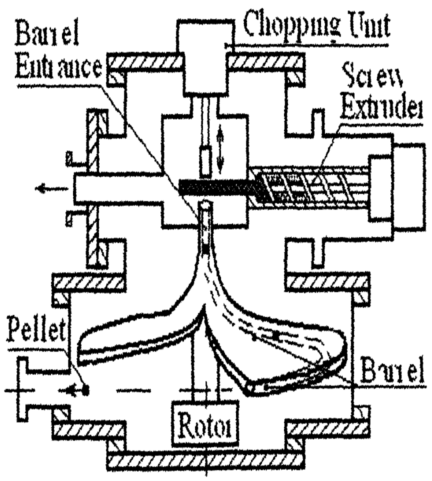

Fig 5 Schematic diagram of a centrifuge pellet injector

Figure is taken from "I.Viniar et al. Fusion Engineering and Design ,59-59, (2001) 295-299"

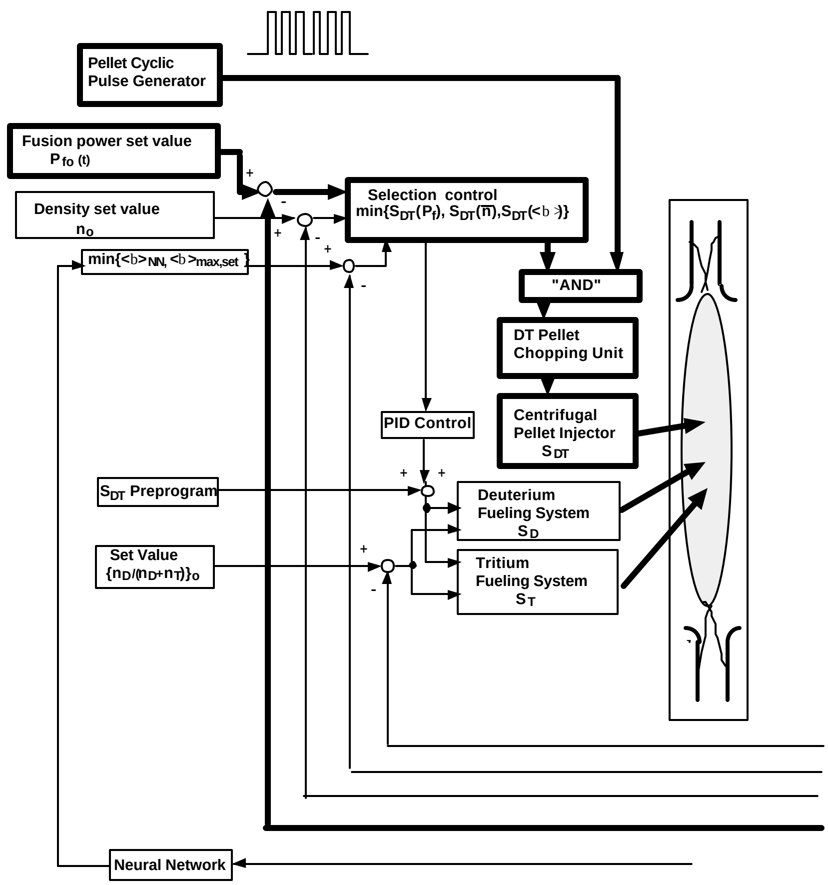

1.8. Calculated results of temporal evolution by pellet injection

(1) Repetitive pellet injection with T_{rep}=0.5 sec and constant gas puffing.

Pellet injection is controlled by the fusion power signal.

$S_{DT}=5\times10^{20}\ m^{-3}/s$ $S_{DT}=4\times10^{20}\ m^{-3}/s$

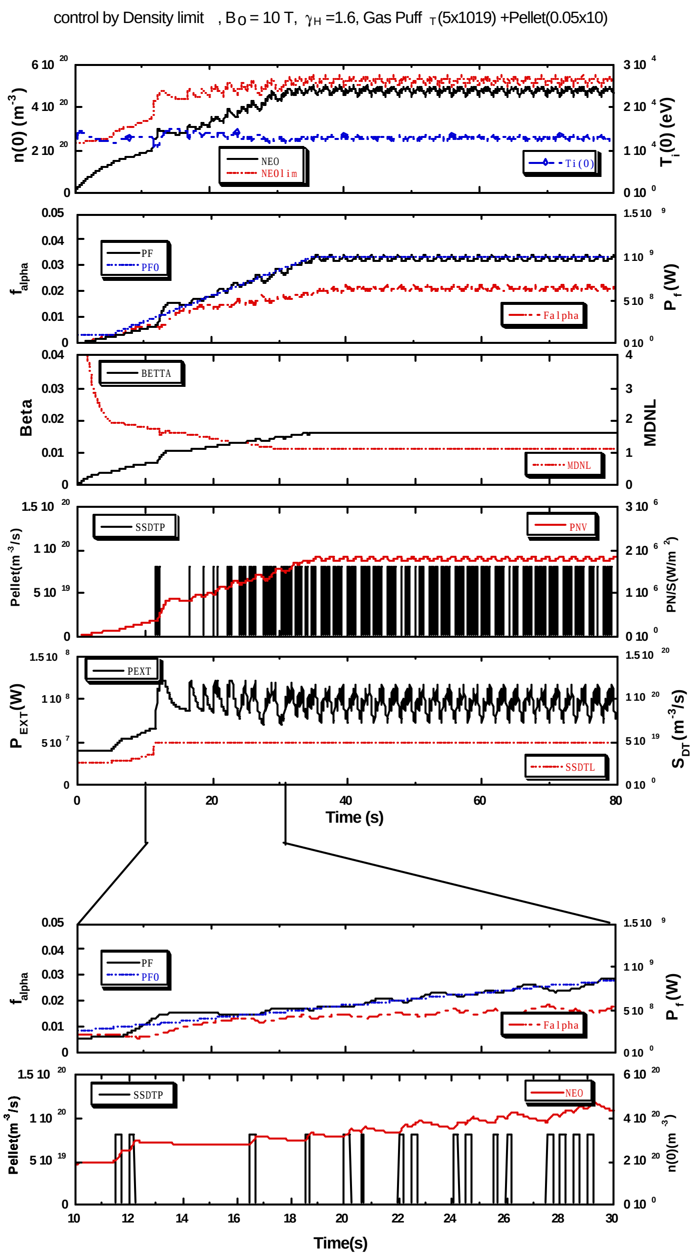

Fig. 4

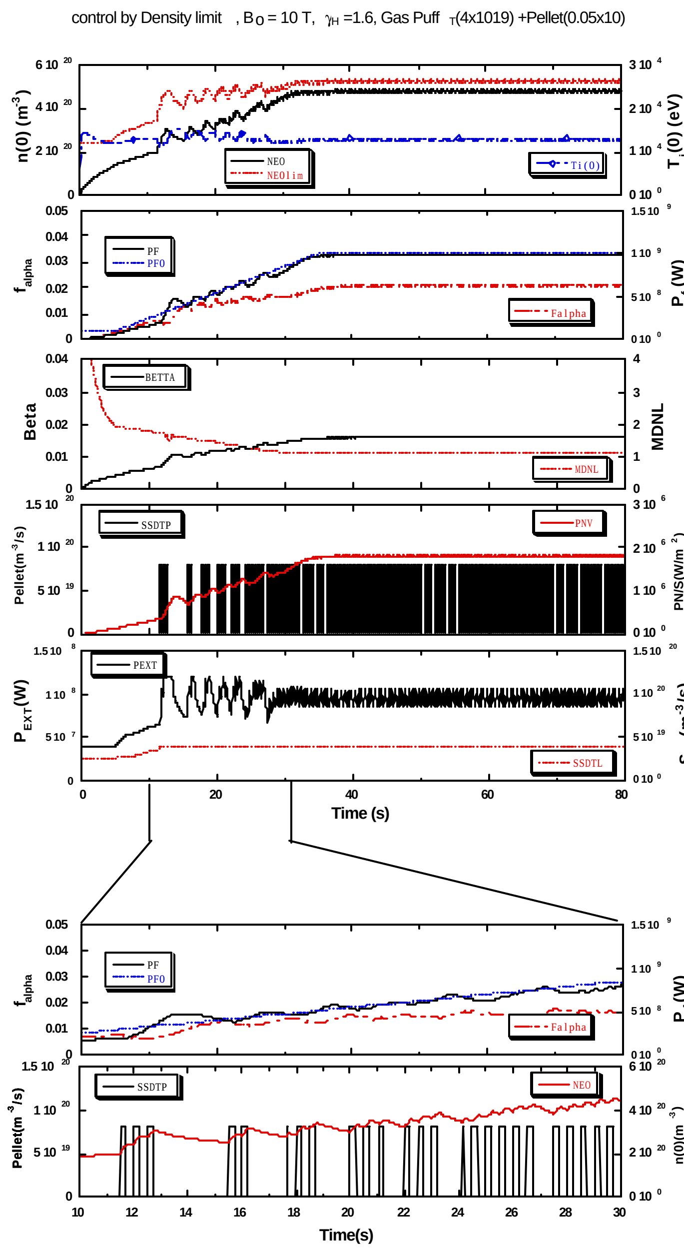

Fig. 3

(2) T_{rep}= 0.2 sec + constant gas puffing

Even if the repetitive pellet injection period is short, the fusion power oscillation cannot be reduced.

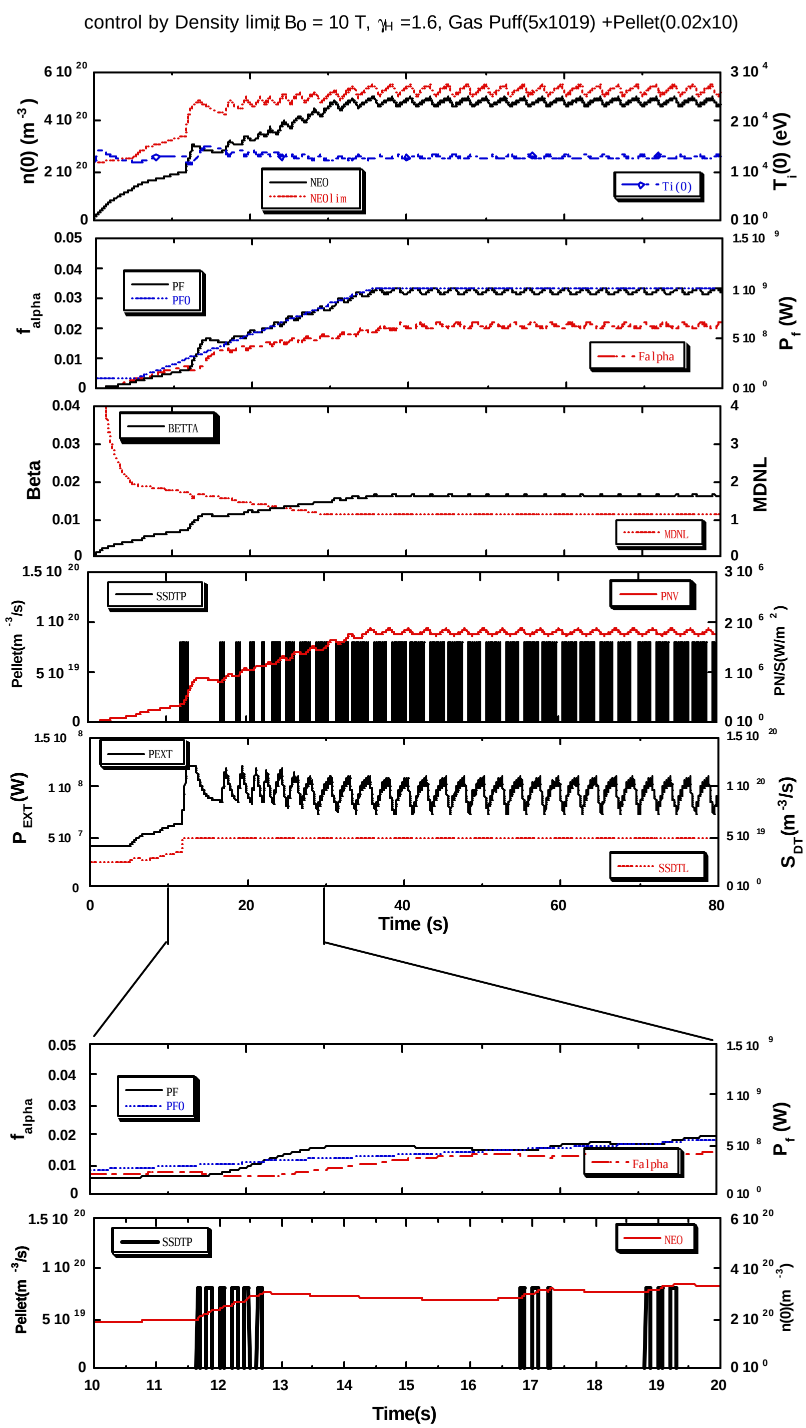

Fig. 8

(3) T_{rep}= 0.5 sec + feedback gas puffing with T_{int} = 30 sec

Pellet injection and gas puffing are both controlled by the fusion power signal. Continuous gas puffing with the long integration time can reduce the fusion power oscillation.

T_{int} = 30 sec

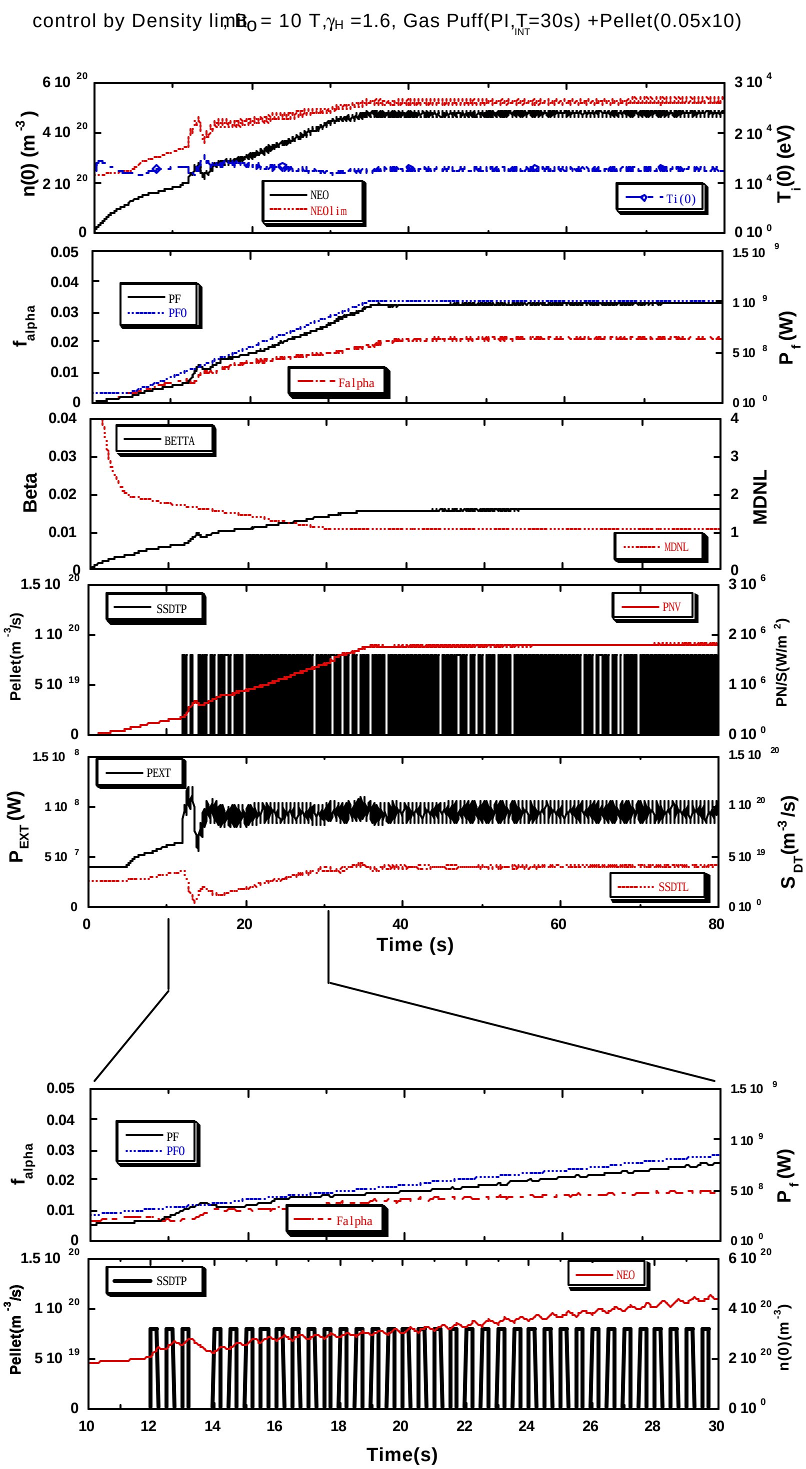

Fig. 1

(4) T_{rep}= 0.5 sec + feedback gas puffing with T_{int} = 20 sec

Shorter integration time cannot reduce the fusion power oscillation. T_{int} = 20 sec

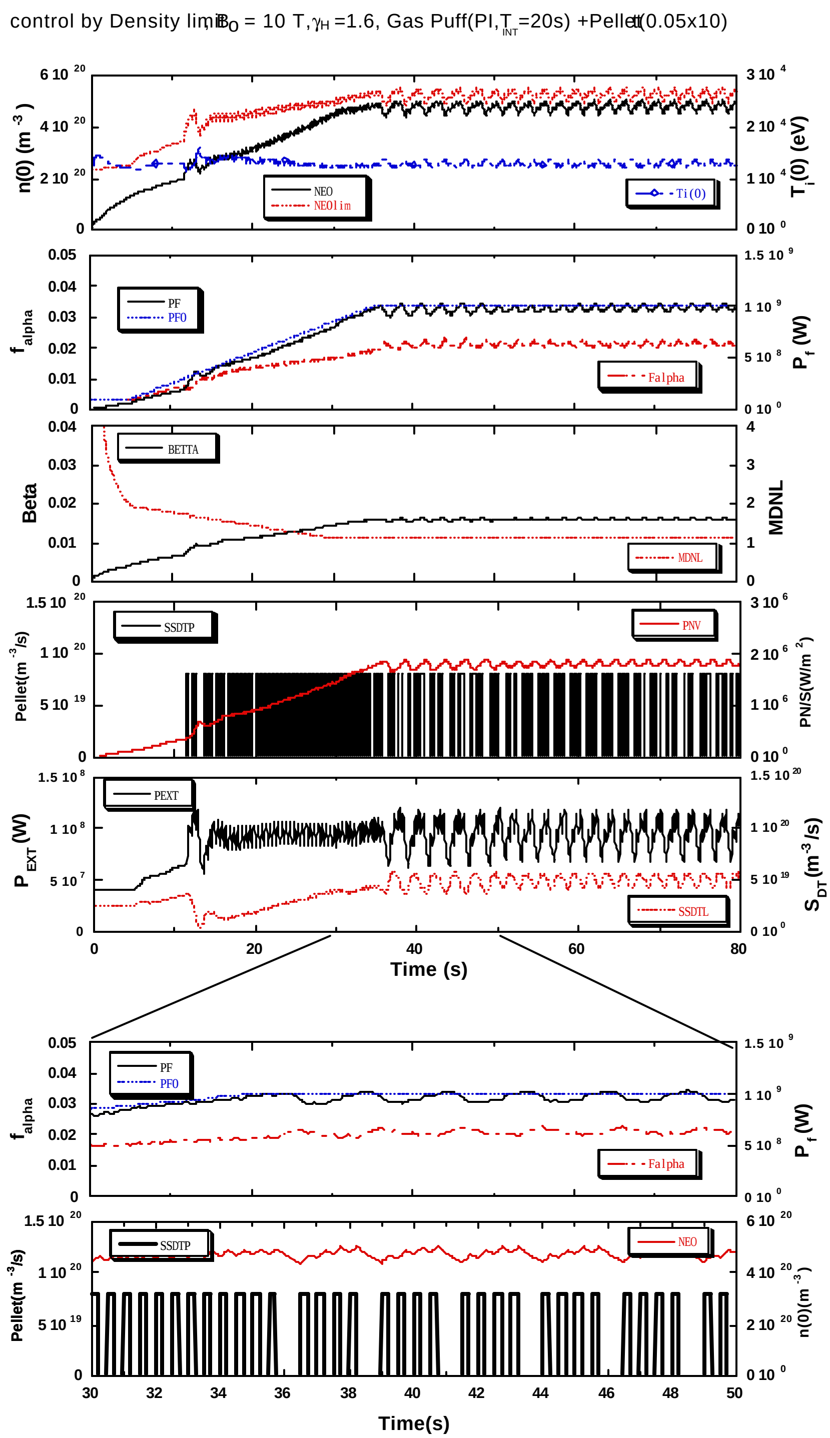

Fig. 2

2. Heat flux ratio at the inboad and outboad first wall

2.1. 3 -dimensional layout

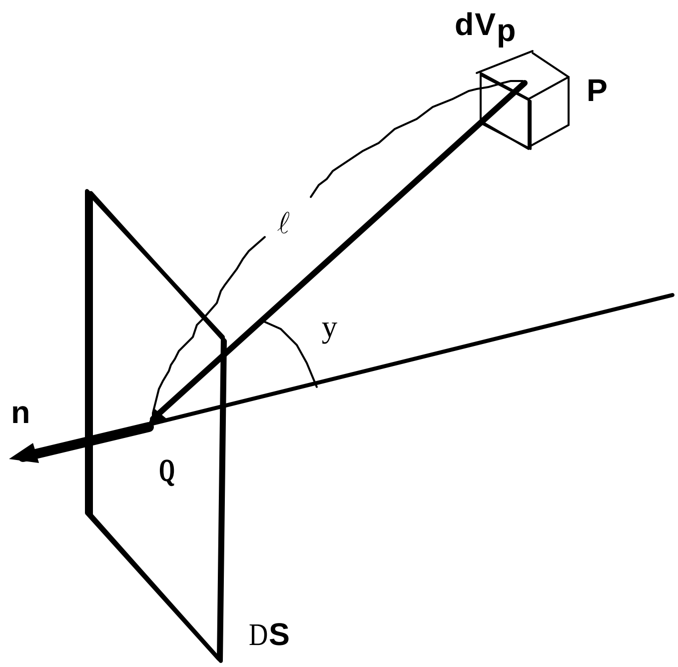

The solid angle on the wall seen from the radiation point P

$$d\Omega = \frac{\cos\psi}{\ell^2}\Delta S \qquad \cos\varphi = \frac{\overline{PQ}\cdot\mathbf{n}}{|\overline{PQ}||\mathbf{n}|}$$

The radiation power received on the first wall with the area ΔS from the radiation in the plasma volume(V_p)

$$Q = \frac{\Delta P}{\Delta S} = \iiint_{V_p} P_b(\rho)\frac{\cos\psi}{4\pi\ell^2}dV_p$$

where P_b is the radiation power per unit volume

$$P_b(\rho) = P_b(0)\left[1 - \left(\frac{\rho}{a_o}\right)^2\right]^{2\alpha_n + 0.5\ \alpha_T}$$

Toroidal coordinate:

$$R = R_o - \rho \cos\theta$$

$$\begin{cases} x_P = R\cos\varphi \\ y_P = R\sin\varphi \\ z_P = \rho\sin\theta \end{cases}$$

$$\begin{cases} x_Q = \rho_{inw} \\ y_Q = 0 \\ z_Q = 0 \end{cases}$$

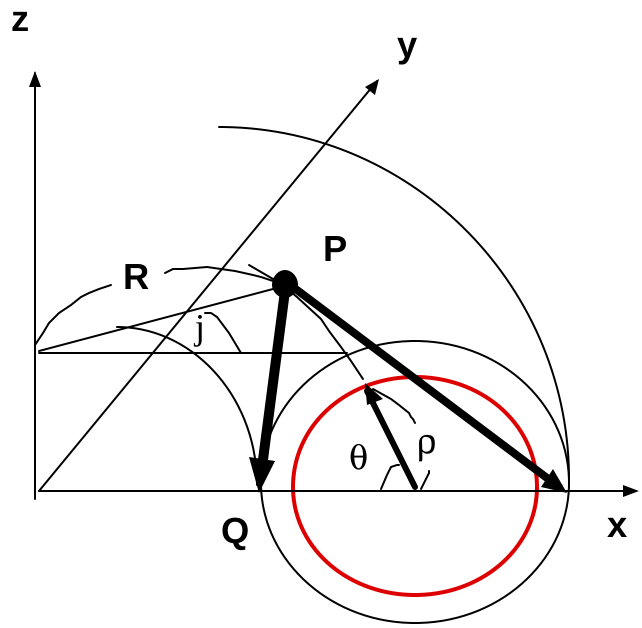

Toroidal coordinate

Heat flux to the inboad surface:

$$\ell_{IN} = \overline{PQ} = \sqrt{(x_P - x_Q)^2 + (y_P - z_Q)^2 + (z_P - z_Q)^2} \qquad \cos\psi_{IN} = \frac{x_P - \rho_{inw}}{\ell}$$

$$\left[Q/P_b(\mathbf{0})\right]_{IN} = \int\!\!\int\!\!\int \left[\frac{\cos\psi_{IN}}{4\pi\,\ell_{IN}^2} \left(1 - \left(\frac{\rho}{a_o}\right)^2\right)^{\left(2\alpha_n + 0.5\alpha_T\right)} \right] \rho d\theta\, d\rho\, R d\varphi$$

Heat flux to the outboad surface:

$$\left[Q/P_b(\mathbf{0})\right]_{OUT} = \int\!\!\int\!\!\int \left[\frac{\cos\psi_{OUT}}{4\pi\,\ell_{OUT}^2} \left(1 - \left(\frac{\rho}{a_o}\right)^2\right)^{\left(2\alpha_n + 0.5\alpha_T\right)} \right] \rho d\theta\, d\rho\, R d\varphi$$

Average heat flux to the outboad surface:

$$\left[Q/P_b(\mathbf{0})\right]_{AVE} = \int\!\!\int\!\!\int \left[\left(1 - \left(\frac{\rho}{a_o}\right)^2\right)^{\left(2\alpha_n + 0.5\alpha_T\right)} \right] \frac{\rho d\theta\, d\rho R d\varphi}{2\pi R\, 2\pi a_w}$$

2.2. Two-dimensional layout

We consider the infinitely long circular tube plasma.

The heat flux with the surface area with DS from the plasma volume(S_p) with unit length

$$Q = \frac{\Delta P}{\Delta S} = \int_{S_p} P_b(\mathbf{r}) \frac{\cos\psi}{2\pi\ell} dS_p$$

Using the x-y components $x = R\cos\varphi$, $y = R\sin\varphi$

$$[Q/P_b(\mathbf{0})]_{IN} = \iint \left[\frac{(x-\rho_{outw})}{(x-\rho_{outw})^2 + y^2} \left(1 - \left(\frac{R-R_o}{a}\right)^2\right)^{(2\alpha_n + 0.5\alpha_T)} \right] \frac{Rd\varphi dR}{2\pi}$$

$$[Q/P_b(\mathbf{0})]_{OUT} = \iint \left[\frac{(\rho_{outw} - x)}{(\rho_{outw} - x)^2 + y^2} \left(1 - \left(\frac{R-R_o}{a}\right)^2\right)^{(2\alpha_n + 0.5\alpha_T)} \right] \frac{Rd\varphi dR}{2\pi}$$

Average heat flux:

$$[Q/P_b(\mathbf{0})]_{AVE} = \iint \left[\left(1 - \left(\frac{R-R_o}{a}\right)^2\right)^{(2\alpha_n + 0.5\alpha_T)} \right] \frac{RdR\, 2\pi L}{S}$$

$$S = 2\pi R_o(2L + 2x2\, a_W) \approx 2\pi R_o 2L$$

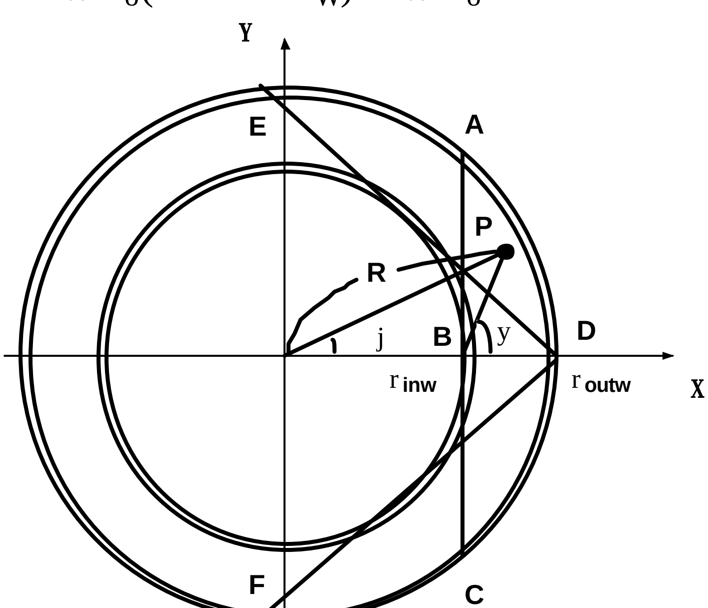

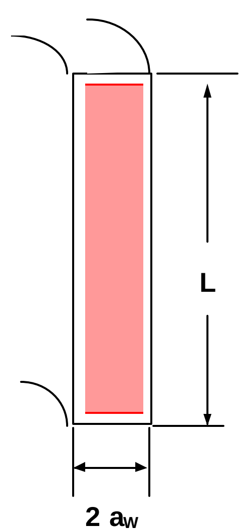

R_o = 10 m, a_o=1 m, a_W=1.2 m, r_{inw} = 8.8 m, r_{outw} = 11.2 m

(1) 2-dimension:

Peaking Factor = Q_{out}/Q_{in}~1.5, Q_{out}/Q_{av}~1.2

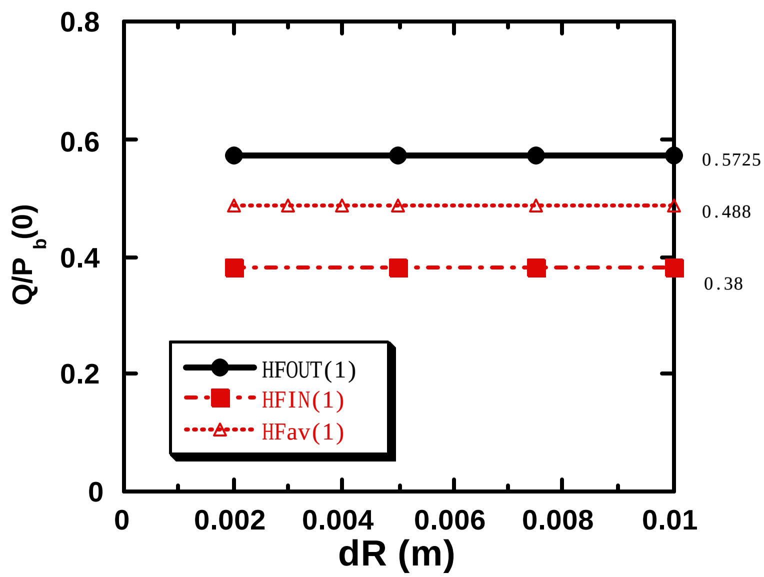

(2) 3-dimension:

Peaking Factor = Q_{out}/Q_{in}~1.1, Q_{out}/Q_{av}~1.03

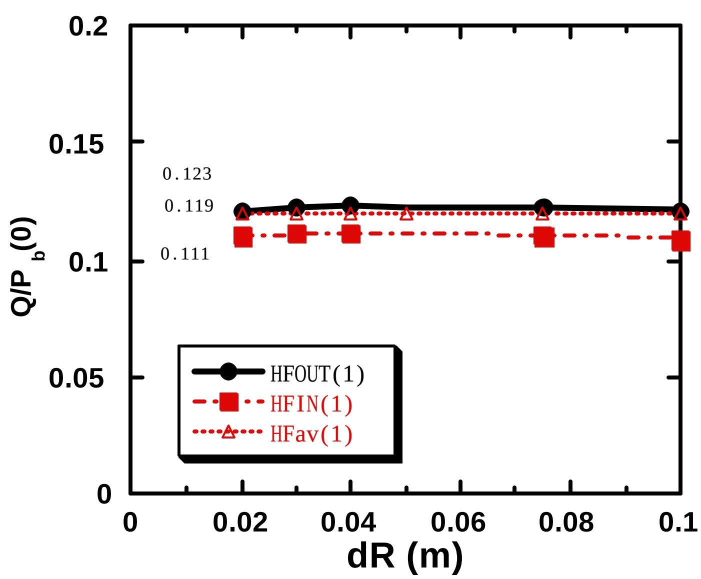

3. Parameter optimization of FFHR

To know the overall behavior of FFHR, the wide parameter regime has been surveyed in terms of

- **machine size R/a,**
- **magnetic field strength B_o,**
- **$Q = P_f/P_{EXT}$, (Ignition --> 1/Q=0)**
- **confinement factor, g_{HH}, over ISS95 scaling**
- **fusion alpha confinement $h_?$(=0.7~1.0),**
- **operating density n.**

R/a=10 m/1.2 m
B_o= 6 T P_f=1GW
P_{EXT}=100MW

R/a=10 m/1 m
B_o= 10 T, P_f=1GW

R/a=10/1.2 m , B_O = 6 T, Gas Puff(PI,T_{INT}=5s)

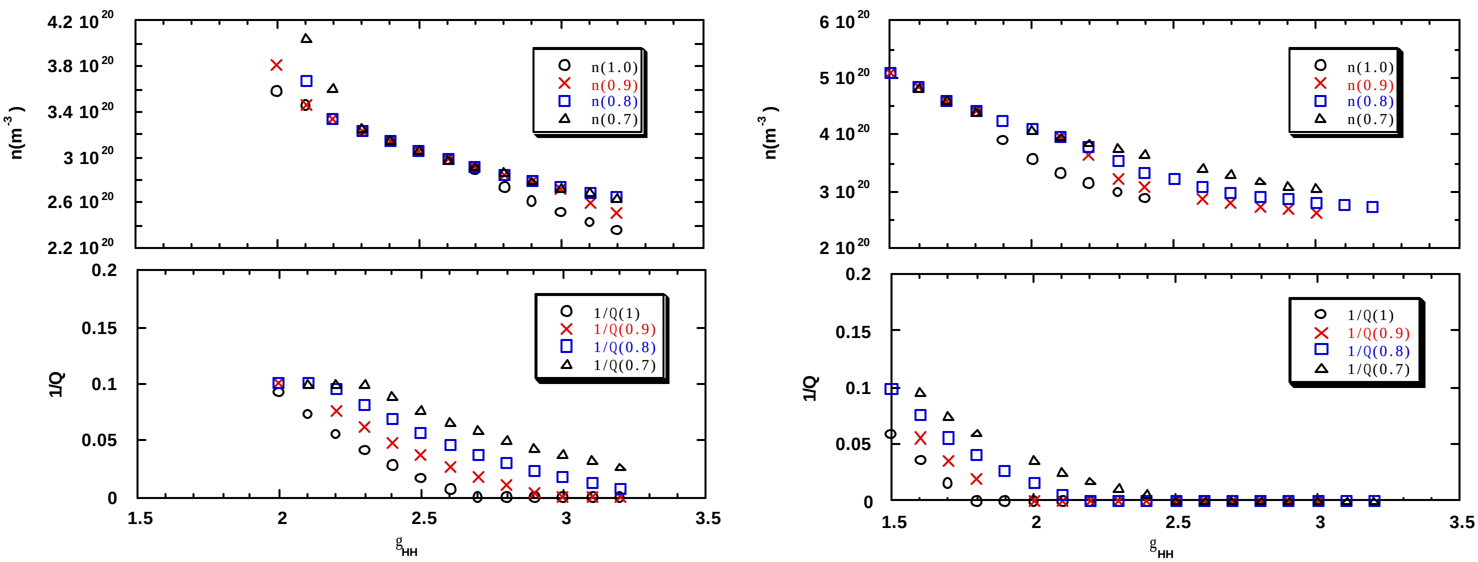

@ In the low field, the confinement factor should be improved by 2 times (g_{HH}=3~3.2) than LHD result to achieve ignition.

@ In the high field, 1.5 times (g_{HH}=2.2~2.4).

In the bigger machine with the low field, the confinement factor should be improved by 1.5 times than that in LHD to achieve ignition. **P_f=3GW, P_{EXT}=100MW**

R/a=15/1.8 m, B_O = 6 T, Gas Puff(PI,T_{INT}=5s)

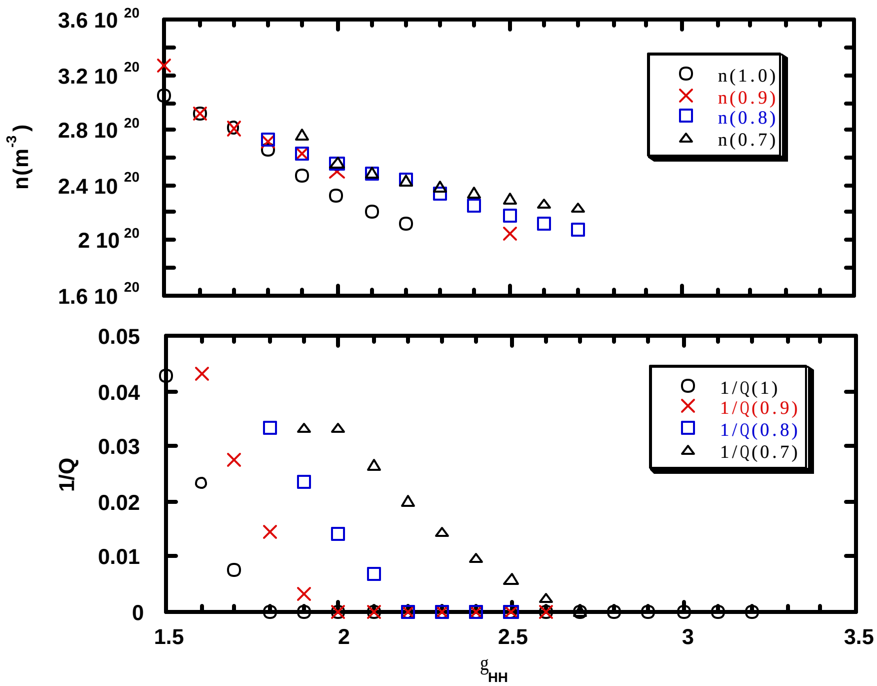

R/a=20/2 m, B_O = 6 T, Gas Puff(PI,T_{INT}=5s)

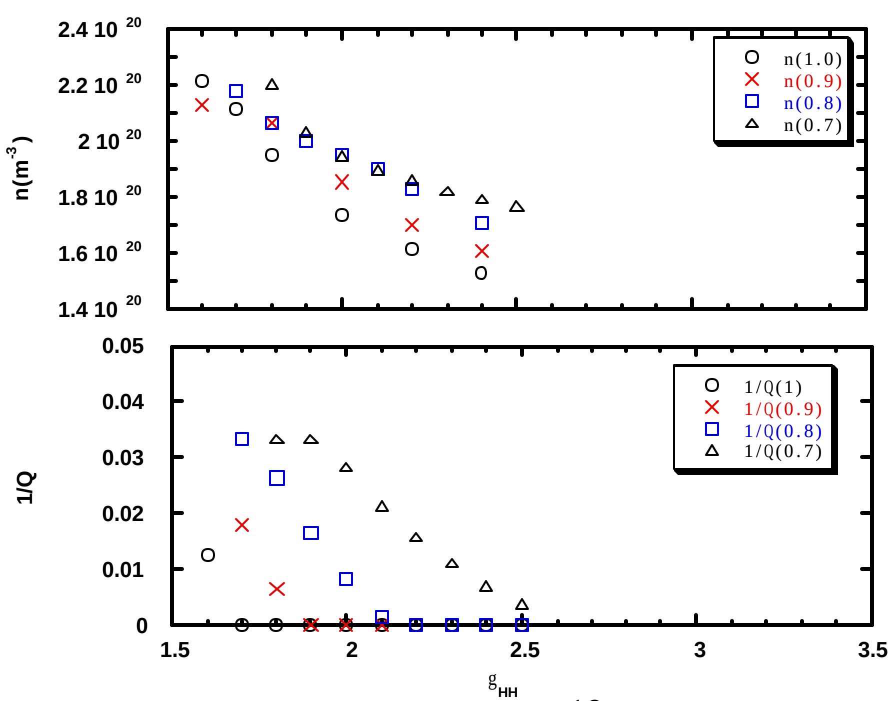

4. Summary and further issues

(1) Assuming the full penetration of pellets into a plasma, subignition access has been studied. The pellet injection control based on the fusion power signal has been demonstrated. In general, the fusion power oscillation takes place when the repetitive pellets are injected.

Even if the repetitive pellet injection period is short, the fusion power oscillation cannot be reduced. The fusion power oscillation can be reduced with the help of the continuous gas puffing with the long integration time even if the repetitive pellet injection period is long.

(2) Global burn control algorithm in a helical reactor has been presented including pellet injection algorithm. Its basic design concept has been proposed.

(3) The ratio of the outboad and average heat flux is 1.2 in two-dimensional layout. In three-dimensional layout, it is smaller as1.03 due to solid angle and "cos" factor. Thus, no large heat flux difference between the outer and inner heat flux is found in FFHR.

In a normal condition, outboard heat flux ~0.08 MW/m^2.

In an abnormal condition, when all the alpha heating power + external heating power are converted to the radiation, the maximum outboard heat flux may reach ~0.8 MW/m^2 in a short time.

Heat flux to the first wall with the elliptic cross section and helical structure should be further examined.

(4) To achieve ignition in a helical reactor, the confinement time should be improved al least by ~1.5 times larger than that in LHD. We need further studies for optimization.